THE JOURNAL OF BIOLOGICAL CHEMISTRY VOL. 289, NO. 26, pp. 18497–18506, June 27, 2014

Error-prone Replication Bypass of the Primary Aflatoxin B_1 DNA Adduct, AFB_1-N7-Gua*

Received for publication, February 26, 2014, and in revised form, May 8, 2014 Published, JBC Papers in Press, May 16, 2014, DOI 10.1074/jbc.M114.561563

Ying-Chih Lin[‡§], Liang Li[¶], Alena V. Makarova[‖], Peter M. Burgers[‖], Michael P. Stone[¶], and R. Stephen Lloyd[§1]**

*From the [‡]Cancer Biology Program, [§]Oregon Institute of Occupational Health Sciences, and **Department of Molecular and Medical Genetics, Oregon Health & Science University, Portland, Oregon 97239, the [¶]Department of Chemistry, Vanderbilt University, Nashville, Tennessee 37235, and the [‖]Department of Biochemistry and Molecular Biophysics, Washington University School of Medicine, St. Louis, Missouri 63110*

Background: Aflatoxin B_1 exposure causes mutations that are associated with liver cancer.
Results: The AFB_1-N7-Gua adduct is highly mutagenic in primate cells, with contributions by both replicative and translesion synthesis DNA polymerases.
Conclusion: AFB_1-N7-Gua adduct is a biologically relevant DNA adduct.
Significance: This is the first study demonstrating the mutagenicity of AFB_1-N7-Gua in mammalian cells and the identification of candidate DNA polymerases involved in these processes.

Hepatocellular carcinomas (HCCs) are the third leading cause of cancer deaths worldwide. The highest rates of early onset HCCs occur in geographical regions with high aflatoxin B_1 (AFB_1) exposure, concomitant with hepatitis B infection. Although the carcinogenic basis of AFB_1 has been ascribed to its mutagenic effects, the mutagenic property of the primary AFB_1-DNA adduct, AFB_1-N7-Gua, in mammalian cells has not been studied extensively. Taking advantage of the ability to create vectors containing a site-specific DNA adduct, the mutagenic potential was determined in primate cells. This adduct was highly mutagenic following replication in COS-7 cells, with a mutation frequency of 45%. The spectrum of mutations was predominantly G to T base substitutions, a result that is consistent with previous mutation data derived from aflatoxin-associated HCCs. To assess which DNA polymerases (pol) might contribute to the mutational outcome, *in vitro* replication studies were performed. Unexpectedly, replicative pol δ and the error-prone translesion synthesis pol ζ were able to accurately bypass AFB_1-N7-Gua. In contrast, replication bypass using pol κ was shown to occur with low fidelity and could account for the commonly detected G to T transversions.

Hepatocellular carcinomas (HCCs)[2] are the most common form of liver cancer and the third leading cause of cancer death worldwide, with about half a million new cases diagnosed each year. Most cases occur in sub-Saharan Africa, Southeast Asia, and China because of the high prevalence of hepatitis B virus (HBV) infection and dietary exposure to aflatoxin B_1 (AFB_1) (1, 2). Chronic exposure to AFB_1 in HBV-infected patients has been shown to correlate with onset of HCC 20 years earlier than in individuals who suffer from HBV infection alone (3). Thus, it is essential to understand the mechanism of action of AFB_1 in hepatocellular carcinogenesis for the development of future effective intervention and therapeutic strategies.

AFB_1 is the most potent hepatocarcinogen of the known natural aflatoxins and is produced as a secondary metabolite by *Aspergillus flavus* and *Aspergillus parasiticus*. These fungi commonly contaminate agricultural crops such as corn and peanuts during their growth in the field and during post-harvest storage (2, 4). Upon ingestion, liver metabolic cytochrome P450 enzymes convert AFB_1 to the reactive intermediate, AFB_1-8,9-epoxide (5, 6), which can conjugate on the N7 atom of deoxyguanosine in DNA to form a quantitatively abundant AFB_1-DNA adduct, 8,9-dihydro-8-(N7-guanyl)-9-hydroxyaflatoxin B_1 (AFB_1-N7-Gua) (see Fig. 1) (7–9). This primary DNA adduct is chemically unstable due to the positive charge on the imidazole ring, which further promotes rearrangement to the open ring form of AFB_1-formamidopyrimidine (AFB_1-FAPY) or depurination to generate an abasic site (AP) (10, 11). Kinetic analyses of the formation and fate of these aflatoxin DNA adducts were determined from rat liver DNA after a single dose exposure. These data revealed that the maximum level of AFB_1-N7-Gua adducts was attained at or before 2 h, with a half-life of 7.5 h. In 24 h, about 20% of the initial AFB_1-N7-Gua was converted to the persistent AFB_1-FAPY adduct, which was continuously detected during the 72-h period studied (12). Thus, the timing of DNA replication in cells relative to the time of the initial adduct formation would significantly determine whether the DNA polymerase (pol) would encounter the AFB_1-N7-Gua, or AFB_1-FAPY adducts, AP sites, or a mixture of all types of DNA lesions.

Mutagenesis that arises from replication of a damaged DNA template in tumor suppressor genes or oncogenes is considered to be the initial step of cancer development. Analyses of two surveys conducted in regions with high prevalence of HBV

* This work was supported by National Institutes of Health Grants R01 CA055678 (to M. P. S. and R. S. L.), GM 032431 (to P. M. B.), and P30 ES00267 (to M. P. S.) and by the OHSU Knight Cancer Institute graduate fellowship (to Y.-C. L.).

[1] To whom correspondence should be addressed. Tel.: 503-494-9957; Fax: 503-494-6831; E-mail: lloydst@ohsu.edu.

[2] The abbreviations used are: HCC, hepatocellular carcinoma; AFB_1, aflatoxin B_1; AFB_1-N7-Gua, 8,9-dihydro-8-(N7-guanyl)-9-hydroxyaflatoxin B_1; FAPY, formamidopyrimidine; ND, nondamaged; ss, single-stranded; TLS, translesion DNA synthesis; pol, DNA polymerase; HBV, hepatitis B virus; AP, abasic site; Exo, exonuclease.

infection and aflatoxin exposure revealed that more than half of the HCC samples contained a G to T mutation at the third position in codon 249 (AGG) of the *p53* tumor suppressor gene (13, 14). This mutation represents a biomarker of aflatoxin exposure as it is not detected in solely HBV-associated HCCs. Multiple experimental mutagenesis studies have shown that the predominant mutation caused by AFB$_1$ exposure is G to T transversion (15–18). Among the three AFB$_1$-induced DNA lesions mentioned above, AP sites appear to make only a minor contribution to the observed G to T mutation in *Escherichia coli* (19). Recently, our group and others have demonstrated that AFB$_1$-FAPY adducts are highly mutagenic precursors in both primate cells and *E. coli* (mutation frequencies of 97 and 32%, respectively), with the G to T transversion being the predominant type of mutation (20, 21). However, the primary AFB$_1$-N7-Gua adducts appear to be only slightly mutagenic in *E. coli*, with an error rate of 4% (19). There are no studies regarding the mutagenic potential of AFB$_1$-N7-Gua in mammalian cells, thus prompting this investigation.

DNA lesions that stall the progression of replication fork can be bypassed using specialized translesion synthesis (TLS) polymerases. However, this bypass may occur at the detriment of genome stability, with the mutation outcome depending on the type of DNA damage and the TLS polymerase utilized (22–24). Recently, pol ζ has been suggested to play a role in replication bypass of AFB$_1$-FAPY adducts, contributing to the predominant G to T transversions (20). There is only limited information regarding how DNA polymerases process the AFB$_1$-N7-Gua adducts. The Klenow fragment (*exo*$^-$) of bacterial DNA pol I could insert either a correct C or a mismatched A opposite AFB$_1$-N7-Gua *in vitro*, but only the mispaired A allowed full-length extension, a result consistent with the observation of G to T mutations (25). In contrast, the archaea *Sulfolobus solfataricus* DNA polymerase IV (Dpo4), a homolog of human pol κ, exhibits error-free bypass of AFB$_1$-N7-Gua *in vitro* (26). The present study was designed to examine the mutagenic potential of AFB$_1$-N7-Gua adducts in primate cells using a site-specific mutagenesis approach and subsequently test the potential role of eukaryotic DNA polymerases in replication bypass of this lesion by *in vitro* replication assays.

EXPERIMENTAL PROCEDURES

Materials—The following materials and reagents were purchased: uracil DNA glycosylase, T4 DNA polymerase, T4 polynucleotide kinase, T4 DNA ligase, and EcoRV (New England Biolabs); [γ-^{32}P]ATP (PerkinElmer Life Sciences); 100 mM dNTPs (GE Healthcare Life Sciences); COS-7 cells (American Type Culture Collection); cell culture media (Dulbecco's modified Eagle's medium and Opti-MEM), Lipofectin transfection reagents, and *E. coli* Max Efficiency DH5α cells (Invitrogen); and human pol κ and ι (Enzymax, LLC). The pMS2 shuttle vector was kindly given by Dr. Masaaki Moriya (State University of New York, Stony Brook, NY). Human pol η catalytic cores were generously given by Dr. Robert Eoff, University of Arkansas (27). WT and the exonuclease-deficient form of pol δ holoenzymes and pol ζ$_4$ (Rev3-Rev7-Pol31-Pol32) of *Saccharomyces cerevisiae* were expressed and purified as described previously (28, 29). Human AP endonuclease was a generous gift from Dr. David Wilson (NIA, National Institutes of Health, Baltimore, MD).

Oligodeoxynucleotides—Oligodeoxynucleotides (5′-ATAATT-*X*AATCC-3′) adducted with AFB$_1$-N7-Gua (see Fig. 1) at the position of *X* were prepared as described previously (6, 30). Nondamaged (ND) oligodeoxynucleotides (12- and 46-mers) with a dG in place of AFB$_1$-N7-Gua and primer DNAs were obtained from Integrated DNA Technologies, Inc. The stability of the AFB$_1$-N7-Gua adduct in the 12-mer oligodeoxynucleotides was tested by assaying for spontaneous depurination. Single-stranded (ss) DNAs were dissolved in a buffer consisting of 10 mM Tris-HCl (pH 7.5) and 1 mM EDTA, and after 3 months, they were digested with human AP endonuclease in 50 mM HEPES, 150 mM KCl, and 2 mM $MgCl_2$. Following electrophoretic separation of the DNAs, there was no evidence of any site-specific depurination of the AFB$_1$-N7-Gua site, suggesting that spontaneous depurination rates are negligible under the storage and manipulation conditions used throughout this study.

Site-specific Mutagenesis in COS-7 Cells—The insertion of modified oligodeoxynucleotide (12-mer) containing an AFB$_1$-N7-Gua adduct into ss pMS2 shuttle vector, cellular transfection, extraction of replicated progeny, and differential hybridization analyses were performed as reported previously (20). Briefly, the 12-mer oligodeoxynucleotide was ligated into an EcoRV-linearized ss pMS2 vector through the complementarity to the center of a 44-mer scaffold DNA (indicated in bold) (5′-CUCGAGGGCCCCUGCAAGCGAU**GGAUUCAAUUA-U**AUCGCUGGUACCGAGCUCGAAUUC-3′), whereas the flanking sequences were annealed to the linearized vector sequences upon EcoRV cleavage of the spontaneous duplex hairpin. Subsequently, the scaffold DNA was removed by uracil DNA glycosylase and T4 DNA polymerase treatments in the absence of dNTPs. Following transfection of site-specifically AFB$_1$-N7-Gua-modified ss pMS2 vector into COS-7 cells, replicated DNAs were extracted and used to transform *E. coli* DH5α cells. Individual colonies were grown in liquid culture and lysed, and then the DNA was cross-linked to a Hybond membrane using a UV Stratalinker.

Differential DNA hybridizations were carried out using a total of four 5′-radiolabeled probes (5′-GATATAATT-*N*AATCCATCGCTT-3′, where *N* refers to G, T, A, or deletion) at 44 °C overnight. To confirm the successful insertion of the 12-mer oligodeoxynucleotides, a bridge probe (5′-ATCCATC-GCTTGCAGGGG-3′) complementary to the sequence at the joint of the vector and insert was used. DNAs that contained the 12-mer insert, but did not hybridize with any of the mutation or deletion probes, were analyzed by DNA sequencing.

Construction of Linear Templates for in Vitro Replication Assay—Linear DNAs (46-mers) modified with AFB$_1$-N7-Gua at a specific site were prepared as reported (20). Briefly, the adducted 12-mer oligodeoxynucleotide was ligated between a 16-mer (5′-ATTATGCAGCGATAGA-3′) and an 18-mer (5′-ATCGCTGGTACCGACTCG-3′) at the 5′ and 3′ ends, respectively, due to their sequential complementarities to a 42-mer scaffold DNA (5′-AGTCGGTACCAGCGATGGATTCAAT-TATTCTATCGCTGCATA-3′). The correctly ligated products were purified by gel electrophoresis. The complete

sequence of the 46-mer was: 5′-ATTATGCAGCGATAGAA-TAATT*X*AATCCATCGCTGGTACCGACTCG-3′, where *X* is AFB$_1$-N7-Gua.

In Vitro DNA Replication Assay—A series of primers whose 3′ end was designed to hybridize upstream (−), opposite (0), or downstream (+) of the lesion site was used to anneal to different regions of the 46-mer template as described previously (20) and shown in the figure insets. Three additional variations of the 0 primer were designed to contain a mismatched nucleotide at the 3′ end (0-A, 0-T, and 0-G primers, respectively). The primers were ^{32}P-labeled and annealed to the 46-mer template at a 1:2 molar ratio in the presence of 40 mM NaCl, heated at 90 °C for 2 min, and cooled to room temperature. The components of the *in vitro* primer extension reactions for pol δ, κ, η, and ι were generally designed from previous studies and included 5 nM primer-template duplex in 25 mM Tris-HCl (pH 7.5), 8 mM $MgCl_2$, 10% glycerol, 100 μg/ml bovine serum albumin, 8 mM NaCl, and 5 mM dithiothreitol (31–33). For pol ζ_4, a different buffer was used, containing 40 mM Tris-HCl, pH 7.6, 0.2 mg/ml bovine serum albumin, 8 mM magnesium acetate, and 120 mM NaCl (29). All the reactions were conducted at 37 °C for 30 min unless specified in the figure legends. Concentrations of dNTP(s) and polymerases are given in the figure legends. An equal volume of a solution containing 95% (v/v) formamide, 20 mM EDTA, 0.02% (w/v) xylene cyanol, and 0.02% (w/v) bromphenol blue was added to terminate the reaction. The reaction products were resolved by electrophoresis through 15% acrylamide denaturing gels containing 8 M urea and visualized by a PhosphorImager screen (GE Healthcare).

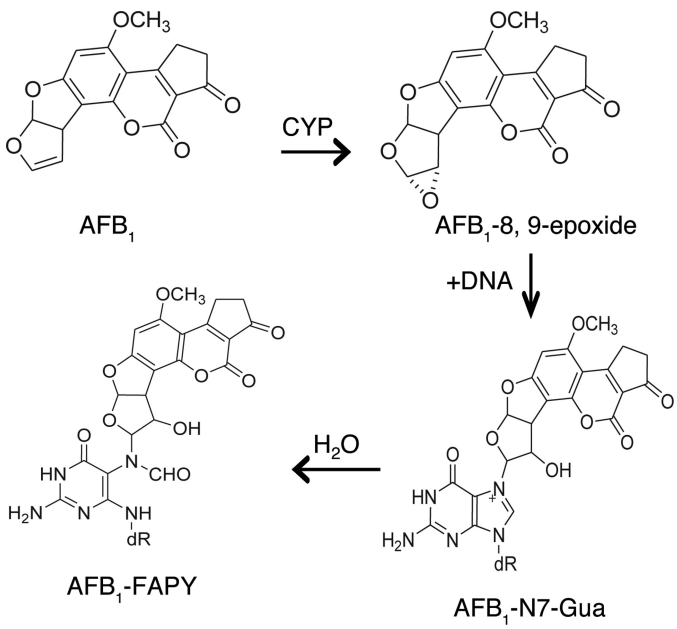

FIGURE 1. **Chemical structures of the AFB$_1$-DNA adducts, adapted from Ref. 20.** *CYP*, cytochrome P450.

RESULTS

Mutagenic Potential of AFB$_1$-N7-Gua Adducts in Primate Cells—To assess whether the AFB$_1$-N7-Gua adducts (Fig. 1) are mutagenic precursors in mammalian cells, we generated an ss shuttle vector pMS2 containing site-specific AFB$_1$-N7-Gua adduct or ND dG control; the vector was subsequently transfected into African green monkey kidney COS-7 cells. The utilization of an ss vector, which was not a suitable substrate for DNA repair, allowed for a reliable determination of the mutagenic frequency and spectra derived from the replication bypass of the lesion. After a 48-h incubation period, the replicated plasmid progenies were extracted and transformed into *E. coli* to form individual colonies. DNAs extracted from bacteria were further hybridized with various DNA probes that were designed to recognize the accurate or mutated sequence at the AFB$_1$-N7-Gua adduct or ND dG insertion region. A bridge probe, spanning both the 12-mer insert and the vector, was used to ensure the successful construction of an ss pMS2 vector containing either AFB$_1$-N7-Gua or ND dG. Thus, a mutagenic spectrum could be inferred through the results of differential hybridization. Representative colonies were picked for DNA sequencing to verify the correct identification of the mutation by each sequence-specific probe. If the bacterial DNA only hybridized with the bridge probe, indicative of the presence of the adducted 12-mer, but not with any sequence-specific mutation probes, plasmid DNAs were extracted for DNA sequencing across the region of the insert to determine the sequence of the progeny DNA. Analyses of these data revealed that replication past the AFB$_1$-N7-Gua adduct resulted in a high error frequency (~45%) (Table 1). No mutations were observed with the control sequence (Table 1). The mutation spectrum included single base substitutions and deletions, with the predominant mutations being G to T transversions, accounting for 82% of all mutations scored. The second most common mutation type was G to A transitions (~10%) followed by G to C transversions and deletions (<3%). Taken together, these data indicate that AFB$_1$-N7-Gua is a highly mutagenic precursor in primate cells, predominantly inducing a G to T transversion, which is consistent with observations of HCC patient samples from areas experiencing high aflatoxin exposure (13, 14).

Accurate Replication Bypass of AFB$_1$-N7-Gua by pol δ—In light of the *in vivo* mutagenesis results, studies were initiated to determine which replicative or TLS DNA polymerases may be involved in synthesis past the AFB$_1$-N7-Gua adducts in COS-7 cells using *in vitro* replication assays. Although the AFB$_1$-FAPY adduct was highly effective in blocking replication

TABLE 1
Mutation spectrum and frequency following replication past AFB$_1$-N7-Gua adducts in COS-7 cells

DNA modification	Colonies scored	Mutated	Single base substitutions			Deletions	Other position substitution	Frequency of mutation (%)
			G to T	G to A	G to C			
ND[a]	189	0	0	0	0	0	0	0
AFB$_1$-N7-Gua	216	98	80 (81.6%)[b]	12 (12.2%)[b]	1 (1%)[b]	3 (3.1%)[b]	2 (2%)[b]	45.4

[a] Replication through nondamaged dG in COS-7 cell, adapted from Ref. 20.
[b] The percentage of total mutated colonies.

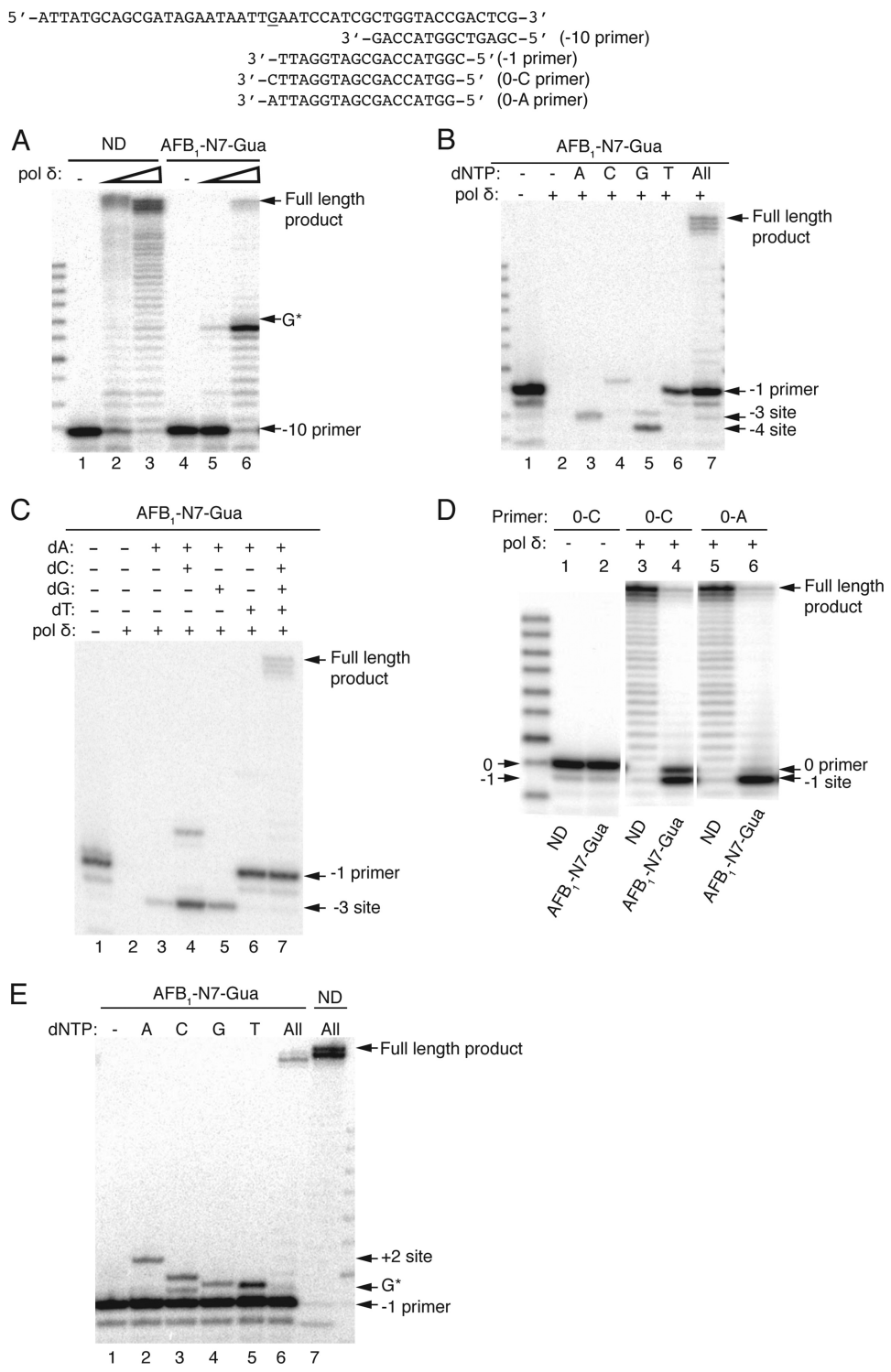

FIGURE 2. **Replication bypass of AFB$_1$-N7-Gua by pol δ.** The −10, −1, or 0 primers with either C or A at the 3′ end were annealed to ND or AFB$_1$-N7-Gua adducted DNA templates. *A*, primer extensions were catalyzed by 1 nM (*lanes 2* and *5*) or 50 nM (*lanes 3* and *6*) pol δ in the presence of 100 μM dNTPs. *G**, adducted site. *B*, single-nucleotide incorporations and primer extensions were conducted by 50 nM pol δ in the presence of combined or individual dNTPs at a final concentration of 100 μM. *C*, dNTP combination and primer extension reactions were catalyzed by 50 nM pol δ in the presence of different combinations of 100 μM individual dNTPs. *D*, primer extensions from the 3′ end of the 0 primer with a matched C or mismatched A annealed opposite ND or AFB$_1$-N7-Gua were catalyzed by 50 nM pol δ in the presence of 100 μM dNTPs in a buffer containing 40 mM Hepes-KOH, pH 6.8, 10% glycerol, 0.2 mg/ml bovine serum albumin, 1 mM DTT, and 8 mM $MgCl_2$ for 1 h at 37 °C. *E*, single-nucleotide insertion opposite AFB$_1$-N7-Gua by pol δ-Exo. Primer extension reactions were catalyzed by 20 nM pol δ-Exo in the presence of 100 μM individual or all dNTPs.

bypass by pol δ (20), it was important to establish whether the ring-closed AFB$_1$-N7-Gua adduct was similarly effective in blocking. Primer extension reactions were carried out using pol δ on control ND or AFB$_1$-N7-Gua-modified templates under running (−10 primer) and standing (−1 primer) start conditions. Under the conditions in which primers annealed to ND

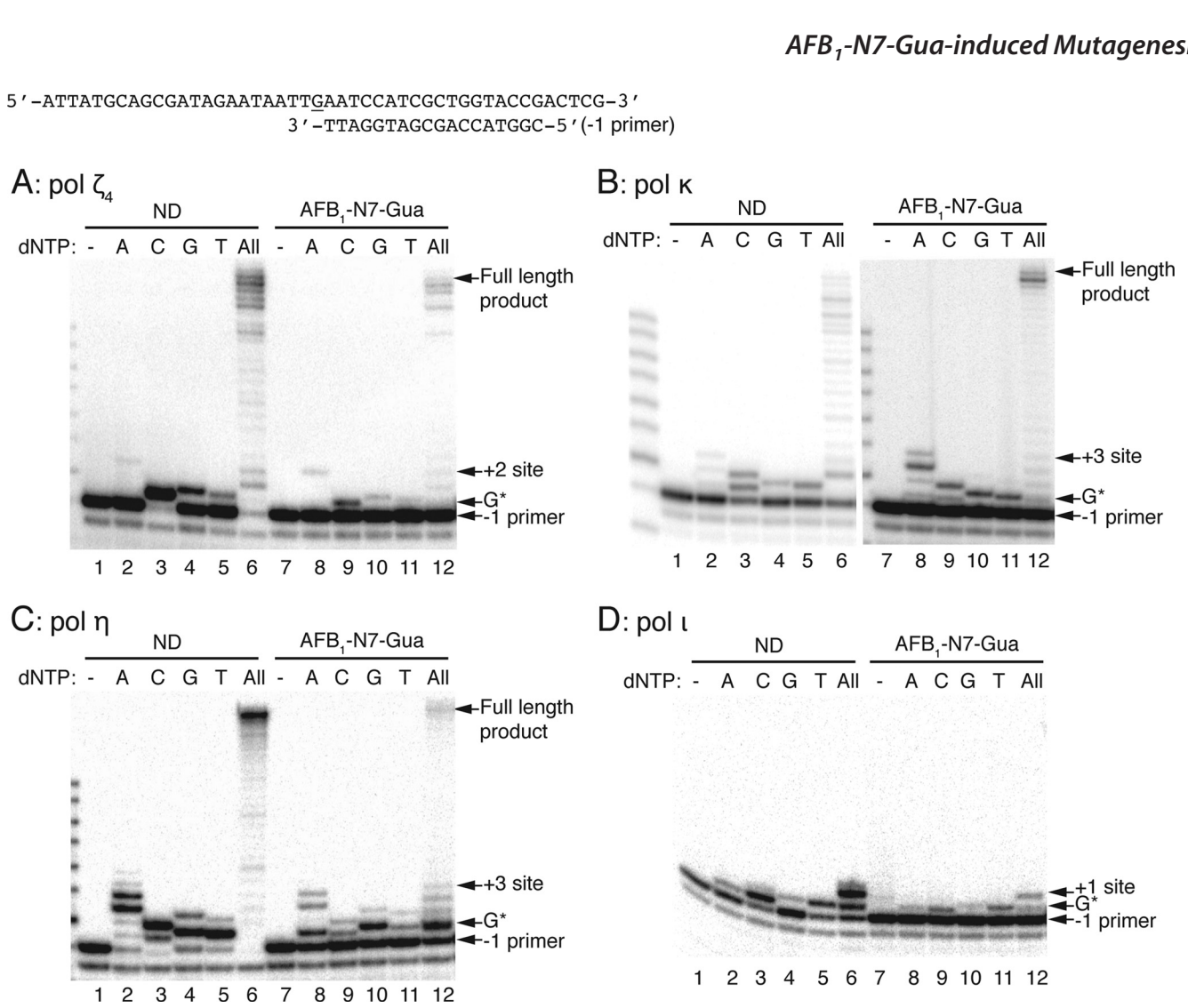

FIGURE 3. **Single-nucleotide incorporations and primer extensions opposite AFB$_1$-N7-Gua by yeast pol ζ_4 and human pol κ, η, and ι.** The −1 primer was annealed to DNA templates containing ND or AFB$_1$-N7-Gua. *A–D*, reactions were catalyzed by 10 nM pol ζ_4, 2 nM (ND) and 10 nM (AFB$_1$-N7-Gua) pol κ, 2 nM pol η catalytic core, and 1 nM pol ι, respectively. 100 μM individual or all dNTPs was used in *panels A* and *B* (AFB$_1$-N7-Gua) and *D*, whereas 20 μM was added in *panels C* and *B* (ND). *G**, adducted site.

templates were efficiently extended, synthesis by pol δ was predominantly inhibited one nucleotide prior to AFB$_1$-N7-Gua (Fig. 2*A*). Surprisingly, unlike comparable replication studies using DNAs containing the AFB$_1$-FAPY adduct, pol δ generated small amounts of full-length bypass product of AFB$_1$-N7-Gua (Fig. 2*A*, *lane 6*). In addition, the presence of the adduct also prevented efficient loading of pol δ at low concentrations, as evidenced by significant reductions in primer utilization (Fig. 2*A*, comparison of *lanes 2* and *5*).

Single-nucleotide incorporation reactions were conducted to determine the specificity of the insertion by pol δ opposite the lesion. As shown in Fig. 2*B*, using the −1 primer, the overall reaction was dominated by the exonucleolytic activity of pol δ (as evidenced by significant degradation of the −1 primers). However, when primer extension was observed, pol δ exclusively inserted the correct C opposite AFB$_1$-N7-Gua, and full-length bypass products were observed in the presence of all dNTPs. In reactions containing only dATP or dGTP, the −1 primer was degraded by the exonuclease proofreading activity of pol δ to −3 or −4 sites, respectively. In the presence of dTTP, primer degradation paused due to polymerase idling at the −1 site. These data suggested that under conditions restricting dNTP availability, the exonuclease reaction dominated the polymerization reaction when pol δ encountered AFB$_1$-N7-Gua adducts. Although these data suggested that pol δ insertion was primarily error-free, an additional experimental strategy was used to corroborate this conclusion. Because the two downstream template nucleotides were both T, it was hypothesized that the addition of dATP with the other individual dNTPs in the reaction could facilitate extension beyond the nucleotide that had been inserted opposite the lesion. As shown in Fig. 2*C*, correct C insertion opposite the lesion followed by incorporation of two additional nucleotides by pol δ was observed, yielding a product band at the +2 site (Fig. 2*C*, *lane 4*). All other permutations of two nucleotides resulted in exonuclease resection back to the nearest complementary nucleotide (Fig. 2*C*, *lanes 3* and *5*). However, when pol δ-Exo was assayed, it inserted all four dNTPs opposite AFB$_1$-N7-Gua and readily extended the misinserted A (Fig. 2*E*), indicating that the presence of the pol δ proofreading function plays a critical role in preventing mutagenesis of AFB$_1$-N7-Gua.

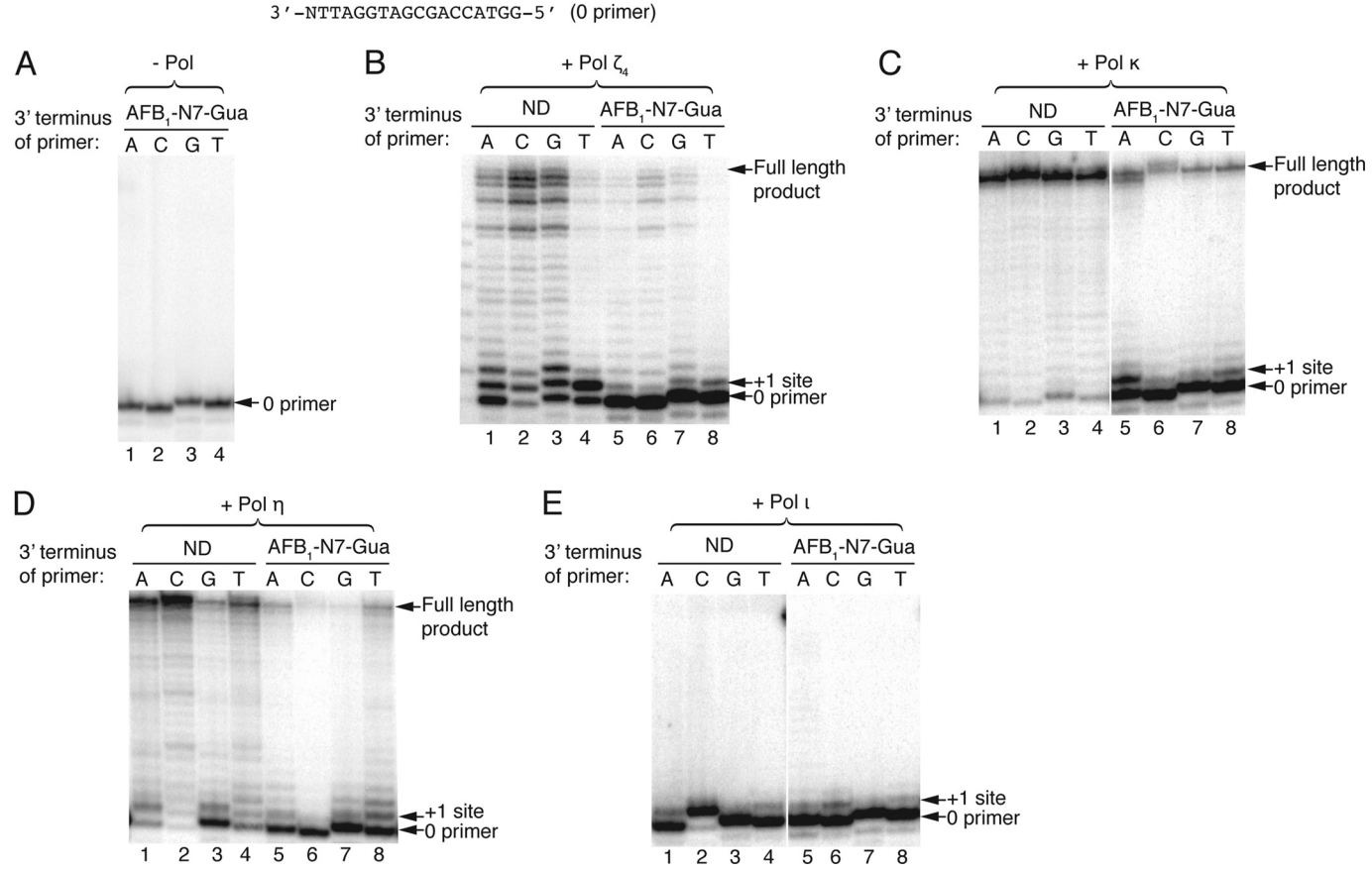

FIGURE 4. **Primer extensions past AFB$_1$-N7-Gua catalyzed by yeast pol ζ_4 and human pol κ, η, and ι.** Four 0 primers with different 3′ ends (where *N* represents A, C, G, or T) were annealed to ND or AFB$_1$-N7-Gua adducted DNA templates. *A*, control reactions contained no polymerase. *B–E*, reactions were catalyzed by 5 nM pol ζ_4, 1 nM pol κ, 0.5 nM pol η, and 10 nM pol ι, respectively. Reactions in *panels A*, *B*, *C*, and *E* were conducted in the presence of 100 μM dNTPs, whereas 20 μM was used in *panel D*.

Although these data suggested that pol δ catalyzed high fidelity replication, the results did not eliminate the possibility that if another polymerase inserted an A opposite the adduct, then pol δ could extend it, contributing to the predominant G to T mutations induced by AFB$_1$-N7-Gua in COS-7 cells (Table 1). To determine whether pol δ was capable of extending a primer constructed with a mispaired A opposite the lesion, as compared with a primer with a matched C, primer extension reactions were carried out. Consistent with the data in Fig. 2, *B* and C, for both primers, the exonucleolytic reaction was more efficient than the extension when replicating through AFB$_1$-N7-Gua. However, the mispaired primer was totally resected to the −1 site (Fig. 2*D*, *lane 6*), whereas the matched C primer was more resistant to the exonuclease processing (Fig. 2*D*, *lane 4*). Although both reactions resulted in full-length products, the abundance was greater for the matched primer. Given the efficiency of the exonucleolytic reaction on the mispaired primer, it is inferred that the full-length products were generated from the resected −1 position.

Thus, these data reveal for the first time that pol δ can replicate past AFB$_1$-N7-Gua by accurate incorporation opposite, and extension beyond, the lesion. These data suggested that pol δ could be involved in limiting mutagenesis of AFB$_1$-N7-Gua *in vivo* and contributing to the error-free portion of the replication (Table 1).

Replication Bypass of AFB$_1$-N7-Gua by TLS Polymerases—Given that nearly 50% of the DNA synthesis past AFB$_1$-N7-Gua in COS-7 cells was mutagenic (Table 1) and that pol δ catalyzed high fidelity bypass of the lesion (Fig. 2), it was hypothesized that one or more of the specialized TLS polymerase(s) may play a role in the AFB$_1$-N7-Gua-induced mutagenesis. To determine the identity of the nucleotide inserted opposite the lesion, single-nucleotide incorporation reactions were carried out with yeast pol ζ_4, human pol κ, η, and ι.

As shown in Fig. 3*A* *lane 9*, pol ζ_4 preferentially inserted the correct C opposite the lesion, whereas A, G, and T were utilized, albeit less efficiently (Fig. 3*A*, *lanes 8*, *10*, and *11*, respectively). With the same experimental approach, pol κ displayed no nucleotide preference (Fig. 3*B*, *lanes 8-11*), whereas pol η preferentially incorporated A and G (Fig. 3*C*). In contrast, pol ι preferred insertion of C and T (Fig. 3*D*).

Given that none of the TLS polymerases tested above exhibited selectivity of insertion of dA opposite the AFB$_1$-N7-Gua adduct, which could play a major role in contributing to the predominant AFB$_1$-N7-Gua-induced G to T mutation, it was hypothesized that TLS polymerases (pols ζ_4, κ, η, and ι) could preferentially extend a mispaired primer opposite the lesion. To experimentally test this, four primers were synthesized such that the 3′-nucleotide represented the matched C and the three mismatches (Fig. 4). Comparative analyses revealed that pol ζ_4

extended the accurate base-paired C primer somewhat more efficiently than any of the other three mispaired primers annealed to the damaged template (Fig. 4*B*).

In the case of pol κ, although full-length bypass products were detected from all four primers hybridized with the damaged template, there was an increased preference for extension from the mispaired A primer (Fig. 4*C*, *lanes 5–8*). However, using conditions to observe these extensions on damaged DNA, all primers were extended on ND templates (Fig. 4*C*, *lanes 1–4*). Similar to that observed for pol κ, pol η preferentially catalyzed primer extension from the mismatched A and T primers for the adducted template (Fig. 4*D*, *lanes 5* and *8*). Moreover, a pol η-deficient COS-7 cell line was made available[3] to test for evidence for a role of pol η in the bypass of this lesion. Using the same site-specific mutagenesis strategy as described above, no differences were observed in the mutation frequency or spectrum in the pol η-defective cells as compared with WT cells. The mutation frequency of AFB$_1$-N7-Gua was 50% in pol η-deficient cells with the predominant mutation type being G to T transversions as 89% of all mutants followed by 11% of G to A transitions.

Consistent with the results obtained for pol ζ_4, pol ι preferentially extended the matched C primers using either the ND or the AFB$_1$-N7-Gua-modified template, albeit inefficiently on the damaged substrate (Fig. 4*E*). In summary, these data provide the first biochemical evidence supporting the possible role of pol ζ_4, in addition to pol δ, in accurate TLS past AFB$_1$-N7-Gua. Pol κ may contribute to misinsertion opposite the adduct and extension from the mispaired A, thus accounting for the predominant G to T mutation in mammalian cells.

Resumption of Efficient Replication by Replicative Polymerase—To address how close to the adduct normal DNA synthesis by replicative polymerase can resume, primer extension reactions were carried out with pol δ using ND or AFB$_1$-N7-Gua modified templates annealed to +2, +3, and +5 primers. These primers contained either matched C or mismatched A opposite the lesion, representing the accurate and mutagenic bypass observed *in vivo*, respectively (Fig. 5). Pol δ extended all primers efficiently when the correct C was paired across control dG or the adduct (Fig. 5*A*, *lanes 4–9*). However, a small percentage of the primer annealed to the templates containing the lesion was resected, primarily back to the +1 site, with slightly higher exonucleolytic activity on the +2 primer. Thus, the extension efficiencies increased as the number of correct base pairs beyond the lesion increased. All primers with the ND template were completely utilized. Conversely, minimal amounts of full-length products were observed when a mispaired A was placed opposite the lesion in the +2 or +3 primer; the exonuclease digested back to the −1 position (Fig. 5*B*, *lanes 7–8*). Interestingly, when the primer terminus was five nucleotides downstream from the mismatched A across the lesion, a substantial amount of full-length extended products was readily detected, with some portion of the +5 primers still excised to the −1 site (Fig. 5*B*, *lane 9*). Moreover, pol δ efficiently extended all the mismatched primers annealed to the ND template (Fig. 5*B*, *lanes 4–6*).

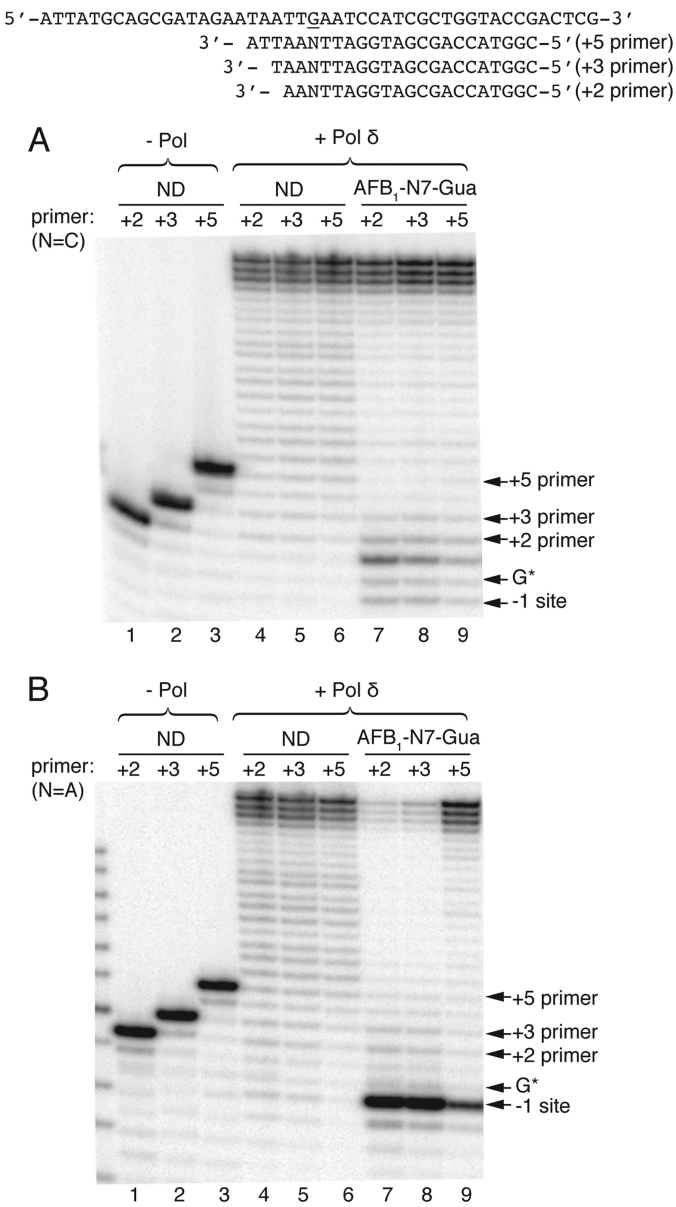

FIGURE 5. **Resumption of replication by pol δ downstream of AFB$_1$-N7-Gua.** +2, +3, or +5 primers with either matched C or mismatched A opposite the lesion or control site were annealed to ND or AFB$_1$-N7-Gua-containing DNA templates. *A* and *B*, primer extensions were catalyzed on matched and mismatched primers, respectively. All reactions were catalyzed by 50 nM pol δ in the presence of 100 μM dNTPs. *G**, adducted site.

In summary, these data revealed that the position of the mispair across the lesion upstream of the primer terminus could affect the DNA synthesis ability of pol δ. The balance between the exonuclease and polymerase activities shifts toward extension when the mismatch was located deeper in the duplex, suggesting the requirement of continuous synthesis by TLS polymerase(s) beyond the lesion to reserve the mutagenic bypass before switching to replicative polymerase.

DISCUSSION

Exposure to aflatoxin, the most potent environmental chemical carcinogen, poses a great risk to public health for the devel-

[3] I. G. Minko, R. W. Sobol, and T. G. Wood, unpublished data.

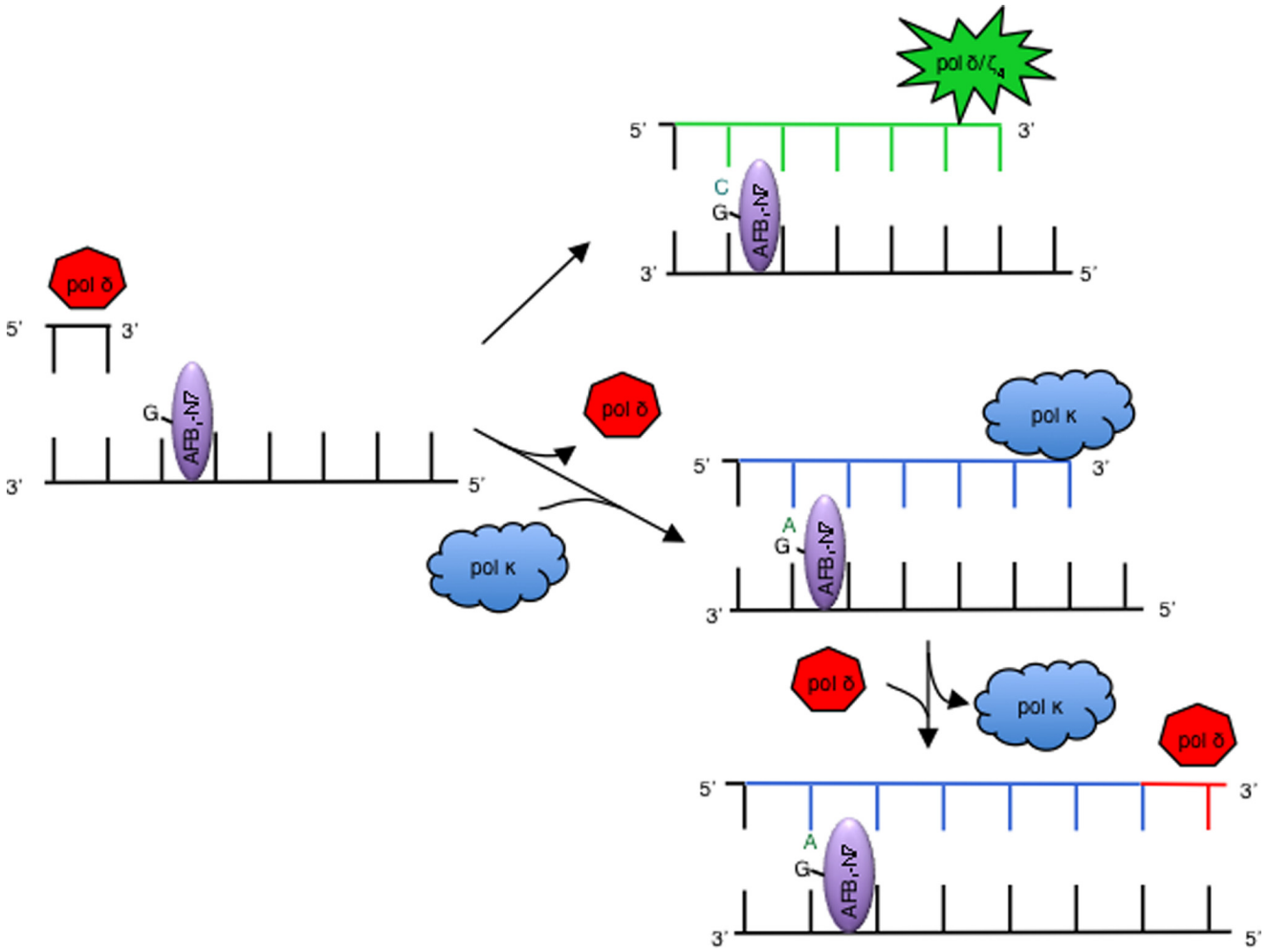

FIGURE 6. **Proposed model of TLS past AFB$_1$-N7-Gua.** The accurate and error-prone bypasses of AFB$_1$-N7-Gua by pol δ or ζ_4 and pol κ, respectively, are shown. For this lesion, the model proposes that pol δ can replicate past the lesion by correct insertion and extension from the damage site. Alternatively, if pol δ is blocked and dissociates one nucleotide prior to the adduct, pol ζ_4 can preferentially insert a correct base opposite and extend from the lesion (*green lines*). The mutagenic pathway involves the blocking of pol δ one nucleotide prior to the lesion followed by recruitment of pol κ to catalyze the insertion step and the more efficient extension from a mispaired A:G terminus (*blue lines*). Efficient resumption of normal replication by pol δ after the second polymerase switch is proposed to occur at least five nucleotides downstream of the mismatched site.

opment of HCCs. About 4.6–28.2% of more than half a million new HCC cases worldwide each year can be attributed to aflatoxin exposure alone (34). Despite intense studies to identify the DNA adducts, mutagenesis, and carcinogenesis induced by aflatoxin, the underlying molecular mechanisms driving these processes are far from completely understood. Recently, we reported that the AFB$_1$-FAPY adducts are highly mutagenic in primate cells (20). The current study utilized exactly the same sequence context- and site-specific mutagenesis approach to demonstrate that the primary AFB$_1$-DNA adduct, AFB$_1$-N7-Gua, was also highly mutagenic (Table 1), although it was about half of that measured for AFB$_1$-FAPY adducts (20). Consistent with the observation made for AFB$_1$-FAPY, the mutagenicity of AFB$_1$-N7-Gua in primate cells was much higher (Table 1) than that in *E. coli* cells (4%) (19). This underscores the advantage of our biologically relevant system to address the mutagenic effects of aflatoxin in animals and humans.

Furthermore, the predominant G to T transversion at the lesion site measured in primate cells was in agreement with that reported in *E. coli* (19). The mutation spectrum also correlated well with other mutagenesis studies in various experimental model systems (15, 17, 18, 35, 36) and aflatoxin-related HCC samples (13, 14). However, no base substitutions located at the 5′ base of AFB$_1$-N7-Gua were detected in our study, suggesting that the mutation at the 5′ base of the lesion identified in *E. coli* (19) could be sequence context-dependent; we can rule out the possible effect of DNA adduct formation and DNA repair on the mutagenesis of this lesion because an ss vector that had been modified by the adduct at a specific site was used. Alternatively, it could also be cell type-specific, considering the differences between primate and SOS-induced bacterial DNA polymerases that may be involved in TLS across AFB$_1$-N7-Gua adducts. Overall, our results support the following conclusions: 1) AFB$_1$-N7-Gua could serve as a mutagenic precursor contributing to the commonly observed G to T transversion as the initiating event of hepatocellular carcinogenesis, and 2) primate cells, and by inference human cells, are more susceptible to the mutagenic effect of AFB$_1$ than *E. coli*, thus providing a basis for AFB$_1$-associated HCC carcinogenesis. We speculate that the data derived from replication of these single-stranded vectors

in African green monkey cells are germane to mutagenic processes in human cells based on a very high degree of sequence identity between human and African green monkey. This assumption is based on unpublished data[4] in which we have cloned and sequenced 16 DNA repair and replication genes from COS-7 cells, and overall, the conservation was 97% for DNA sequence and 98% for amino acid identity.

A model of TLS past AFB$_1$-N7-Gua adducts was inferred based on the biochemical studies (Fig. 6). High fidelity replication bypass of the AFB$_1$-N7-Gua adduct occurred in about half of the progeny, and these data are consistent with a bypass mechanism mediated by pol δ or pol ζ_4 (Fig. 6, *left*). If, however, the AFB$_1$-N7-Gua adduct causes blockage of the replicative polymerase, this could lead to the recruitment of pol κ that would subsequently catalyze incorporation of all dNTPs opposite the lesion and preferentially extend the mismatched dA (Fig. 6, *right*). We favor this explanation to account for the G to T transversion over a slippage realignment model, in which the 5′-dT would be used as the template for the exclusive insertion of dA. The insertion of all dNTPs equally by pol κ without preference for dA (Fig. 3*B*) argues against the slippage realignment model; instead, the preferential extension off of dA by pol κ could potentially account for the observed mutagenesis. These results will aid us in focusing future studies into the biological role of these polymerases in the bypass of AFB$_1$-DNA adducts.

Although both AFB$_1$-N7-Gua and AFB$_1$-FAPY adducts intercalate at the 5′ face of the modified base in duplex DNA (37, 38), potentially explaining the similar mutation spectrum, with predominant mutation being G to T transversion, it does not provide insight for the differential mutagenic potential between these two lesions (Table 1) (20). Recently, crystallographic studies revealed that the conformation of the AFB$_1$ moiety within the active site of the archaea polymerase Dpo4 differed between AFB$_1$-N7-Gua and AFB$_1$-FAPY due to the distinct orientations of the N7–C8 bond of AFB$_1$-N7-Gua as compared with the N^5–C8 bond of AFB$_1$-FAPY (26). To keep the N7–C8 bond of AFB$_1$-N7-Gua in plane with the adducted dG, the AFB$_1$ moiety of AFB$_1$-N7-Gua is 16° out of plane relative to the modified dG, forming a wedge in the DNA; this is believed to allow better access for the incoming dCTP (26). This could be a plausible mechanism underlying the more accurate bypass of AFB$_1$-N7-Gua that was observed in this study. However, bacterial DNA pol I Klenow *exo*$^-$ has been shown to be capable of inserting both dA and dC opposite AFB$_1$-N7-Gua, with the exclusive extension from the mispaired primer template (25). Thus, it warrants further investigation of crystal structures of these eukaryotic polymerases in complex with AFB$_1$-N7-Gua adducts to elucidate the mechanisms that may contribute to the mutagenic outcome in mammalian cells.

In the current study, we established that AFB$_1$-N7-Gua lesions are biologically relevant DNA adducts causing primarily G to T transversions, the predominant mutation induced by AFB$_1$ exposure, in primate cells. Furthermore, biochemical evidence of DNA replication bypass of these adducts was provided, and from this, attention could be focused particularly on pol δ, ζ, and κ for *in vivo* assays to advance our understanding of cellular pathways that involve in AFB$_1$-induced mutagenesis as the initiation of AFB$_1$-related HCC.

Acknowledgments—We thank Dr. Masaaki Moriya (State University of New York at Stony Brook) for the generous gift of pMS2 vector, Dr. Irina G. Minko (Oregon Health & Science University) for critical discussions throughout the course of these studies and preparation of ss pMS2, Lauriel F. Earley for technical support, Dr. Robert Eoff (University of Arkansas) for the generous gift of pol η catalytic core, and Dr. David M. Wilson III (NIA, National Institutes of Health) for the kind gift of human AP endonuclease. We also thank Drs. Robert W. Sobol (University of Pittsburgh), Thomas G. Wood (University of Texas Medical Branch), and Irina G. Minko for contributions to creating stable knockdowns of DNA polymerase η in COS-7 cells.

REFERENCES

1. Ferlay, J., Shin, H.-R., Bray, F., Forman, D., Mathers, C., and Parkin, D. M. (2010) Estimates of worldwide burden of cancer in 2008: GLOBOCAN 2008. *Int. J. Cancer* **127,** 2893–2917
2. McGlynn, K. A., and London, W. T. (2011) The global epidemiology of hepatocellular carcinoma: present and future. *Clin. Liver Dis.* **15,** 223–243, vii–x
3. Kensler, T. W., Qian, G.-S., Chen, J. G., and Groopman, J. D. (2003) Translational strategies for cancer prevention in liver. *Nat. Rev. Cancer* **3,** 321–329
4. Roze, L. V., Hong, S.-Y., and Linz, J. E. (2013) Aflatoxin biosynthesis: current frontiers. *Annu. Rev. Food Sci. Technol.* **4,** 293–311
5. Forrester, L. M., Neal, G. E., Judah, D. J., Glancey, M. J., and Wolf, C. R. (1990) Evidence for involvement of multiple forms of cytochrome P-450 in aflatoxin B$_1$ metabolism in human liver. *Proc. Natl. Acad. Sci. U.S.A.* **87,** 8306–8310
6. Baertschi, S. W., Raney, K. D., Stone, M. P., and Harris, T. M. (1988) Preparation of the 8,9-epoxide of the mycotoxin aflatoxin B$_1$: the ultimate carcinogenic species. *J. Am. Chem. Soc.* **110,** 7929–7931
7. Martin, C. N., and Garner, R. C. (1977) Aflatoxin B-oxide generated by chemical or enzymic oxidation of aflatoxin B1 causes guanine substitution in nucleic acids. *Nature* **267,** 863–865
8. Essigmann, J. M., Croy, R. G., Nadzan, A. M., Busby, W. F., Jr., Reinhold, V. N., Büchi, G., and Wogan, G. N. (1977) Structural identification of the major DNA adduct formed by aflatoxin B$_1$ *in vitro*. *Proc. Natl. Acad. Sci. U.S.A.* **74,** 1870–1874
9. Croy, R. G., Essigmann, J. M., Reinhold, V. N., and Wogan, G. N. (1978) Identification of the principal aflatoxin B$_1$-DNA adduct formed *in vivo* in rat liver. *Proc. Natl. Acad. Sci. U.S.A.* **75,** 1745–1749
10. Groopman, J. D., Croy, R. G., and Wogan, G. N. (1981) *In vitro* reactions of aflatoxin B1-adducted DNA. *Proc. Natl. Acad. Sci. U.S.A.* **78,** 5445–5449
11. Brown, K. L., Deng, J. Z., Iyer, R. S., Iyer, L. G., Voehler, M. W., Stone, M. P., Harris, C. M., and Harris, T. M. (2006) Unraveling the aflatoxin-FAPY conundrum: structural basis for differential replicative processing of isomeric forms of the formamidopyrimidine-type DNA adduct of aflatoxin B$_1$. *J. Am. Chem. Soc.* **128,** 15188–15199
12. Croy, R. G., and Wogan, G. N. (1981) Temporal patterns of covalent DNA adducts in rat liver after single and multiple doses of aflatoxin B$_1$. *Cancer Res.* **41,** 197–203
13. Hsu, I. C., Metcalf, R. A., Sun, T., Welsh, J. A., Wang, N. J., and Harris, C. C. (1991) Mutational hotspot in the p53 gene in human hepatocellular carcinomas. *Nature* **350,** 427–428
14. Bressac, B., Kew, M., Wands, J., and Ozturk, M. (1991) Selective G to T mutations of p53 gene in hepatocellular carcinoma from southern Africa. *Nature* **350,** 429–431
15. Foster, P. L., Eisenstadt, E., and Miller, J. H. (1983) Base substitution mutations induced by metabolically activated aflatoxin B$_1$. *Proc. Natl. Acad. Sci. U.S.A.* **80,** 2695–2698

[4] R. S. Lloyd, I. G. Minko, and T. G. Wood, unpublished data.

16. Chang, Y. J., Mathews, C., Mangold, K., Marien, K., Hendricks, J., and Bailey, G. (1991) Analysis of *ras* gene mutations in rainbow trout liver tumors initiated by aflatoxin B_1. *Mol. Carcinog.* **4,** 112–119
17. Levy, D. D., Groopman, J. D., Lim, S. E., Seidman, M. M., and Kraemer, K. H. (1992) Sequence specificity of aflatoxin B_1-induced mutations in a plasmid replicated in xeroderma pigmentosum and DNA repair proficient human cells. *Cancer Res.* **52,** 5668–5673
18. Aguilar, F., Hussain, S. P., and Cerutti, P. (1993) Aflatoxin B_1 induces the transversion of G → T in codon 249 of the p53 tumor suppressor gene in human hepatocytes. *Proc. Natl. Acad. Sci. U.S.A.* **90,** 8586–8590
19. Bailey, E. A., Iyer, R. S., Stone, M. P., Harris, T. M., and Essigmann, J. M. (1996) Mutational properties of the primary aflatoxin B_1-DNA adduct. *Proc. Natl. Acad. Sci. U.S.A.* **93,** 1535–1539
20. Lin, Y.-C., Li, L., Makarova, A. V., Burgers, P. M., Stone, M. P., and Lloyd, R. S. (2014) Molecular basis of aflatoxin-induced mutagenesis: role of the aflatoxin B1-formamidopyrimidine adduct. *Carcinogenesis*, in press
21. Smela, M. E., Hamm, M. L., Henderson, P. T., Harris, C. M., Harris, T. M., and Essigmann, J. M. (2002) The aflatoxin B_1 formamidopyrimidine adduct plays a major role in causing the types of mutations observed in human hepatocellular carcinoma. *Proc. Natl. Acad. Sci. U.S.A.* **99,** 6655–6660
22. Lange, S. S., Takata, K., and Wood, R. D. (2011) DNA polymerases and cancer. *Nat. Rev. Cancer* **11,** 96–110
23. Sale, J. E., Lehmann, A. R., and Woodgate, R. (2012) Y-family DNA polymerases and their role in tolerance of cellular DNA damage. *Nat. Rev. Mol. Cell Biol.* **13,** 141–152
24. Yamanaka, K., and Lloyd, R. S. (2013) in *DNA Repair and Cancer: From Bench to Clinic* (Madhusudan, S., and Wilson, D. M., III, eds) pp. 325–371, CRC Press, Boca Raton, FL
25. Johnston, D. S., and Stone, M. P. (2000) Replication of a site-specific *trans*-8,9-dihydro-8-(N7-guanyl)-9-hydroxyaflatoxin B_1 adduct by the exonuclease deficient Klenow fragment of DNA polymerase I. *Chem. Res. Toxicol.* **13,** 1158–1164
26. Banerjee, S., Brown, K. L., Egli, M., and Stone, M. P. (2011) Bypass of aflatoxin B_1 adducts by the *Sulfolobus solfataricus* DNA polymerase IV. *J. Am. Chem. Soc.* **133,** 12556–12568
27. Maddukuri, L., Ketkar, A., Eddy, S., Zafar, M. K., Griffin, W. C., and Eoff, R. L. (2012) Enhancement of human DNA polymerase η activity and fidelity is dependent upon a bipartite interaction with the Werner syndrome protein. *J. Biol. Chem.* **287,** 42312–42323
28. Jin, Y. H., Garg, P., Stith, C. M. W., Al-Refai, H., Sterling, J. F., Murray, L. J. W., Kunkel, T. A., Resnick, M. A., Burgers, P. M., and Gordenin, D. A. (2005) The multiple biological roles of the 3′→5′ exonuclease of *Saccharomyces cerevisiae* DNA polymerase δ require switching between the polymerase and exonuclease domains. *Mol. Cell. Biol.* **25,** 461–471
29. Makarova, A. V., Stodola, J. L., and Burgers, P. M. (2012) A four-subunit DNA polymerase ζ complex containing Pol δ accessory subunits is essential for PCNA-mediated mutagenesis. *Nucleic Acids Res.* **40,** 11618–11626
30. Gopalakrishnan, S., Stone, M. P., and Harris, T. M. (1989) Preparation and characterization of an aflatoxin B_1 adduct with the oligodeoxynucleotide $d(ATCGAT)_2$. *J. Am. Chem. Soc.* **111,** 7232–7239
31. Yamanaka, K., Minko, I. G., Finkel, S. E., Goodman, M. F., and Lloyd, R. S. (2011) Role of high-fidelity *Escherichia coli* DNA polymerase I in replication bypass of a deoxyadenosine DNA-peptide cross-link. *J. Bacteriol.* **193,** 3815–3821
32. Minko, I. G., Harbut, M. B., Kozekov, I. D., Kozekova, A., Jakobs, P. M., Olson, S. B., Moses, R. E., Harris, T. M., Rizzo, C. J., and Lloyd, R. S. (2008) Role for DNA polymerase κ in the processing of N2-N2-guanine interstrand cross-links. *J. Biol. Chem.* **283,** 17075–17082
33. Fernandes, P. H., and Lloyd, R. S. (2007) Mutagenic bypass of the butadiene-derived 2′-deoxyuridine adducts by polymerases η and ζ. *Mutat Res.* **625,** 40–49
34. Liu, Y., and Wu, F. (2010) Global burden of aflatoxin-induced hepatocellular carcinoma: a risk assessment. *Environ. Health Perspect.* **118,** 818–824
35. Besaratinia, A., Kim, S.-I., Hainaut, P., and Pfeifer, G. P. (2009) *In vitro* recapitulating of TP53 mutagenesis in hepatocellular carcinoma associated with dietary aflatoxin B1 exposure. *Gastroenterology* **137,** 1127–1137
36. Wattanawaraporn, R., Woo, L. L., Belanger, C., Chang, S.-C., Adams, J. E., Trudel, L. J., Bouhenguel, J. T., Egner, P. A., Groopman, J. D., Croy, R. G., Essigmann, J. M., and Wogan, G. N. (2012) A single neonatal exposure to aflatoxin b_1 induces prolonged genetic damage in two loci of mouse liver. *Toxicol. Sci.* **128,** 326–333
37. Gopalakrishnan, S., Harris, T. M., and Stone, M. P. (1990) Intercalation of aflatoxin B_1 in two oligodeoxynucleotide adducts: comparative ^{1}H NMR analysis of $d(ATC^{AFB}GAT).d(ATCGAT)$ and $d(AT^{AFB}GCAT)_2$. *Biochemistry* **29,** 10438–10448
38. Mao, H., Deng, Z., Wang, F., Harris, T. M., and Stone, M. P. (1998) An intercalated and thermally stable FAPY adduct of aflatoxin B_1 in a DNA duplex: structural refinement from ^{1}H NMR. *Biochemistry* **37,** 4374–4387